

Lower relative abundance of ectomycorrhizal fungi under a warmer and drier climate is linked to enhanced soil organic matter decomposition

José Ignacio Querejeta^{1*} , Klaus Schlaeppi^{2,3,4} , Álvaro López-García⁵ , Sara Ondoño¹ , Iván Prieto¹ , Marcel G. A. van der Heijden^{2,6,7}  and María del Mar Alguacil^{5*} 

¹Department of Soil and Water Conservation (CEBAS-CSIC), CSIC-Centro de Edafología y Biología Aplicada del Segura, PO Box 164, Campus de Espinardo, 30100 Murcia, Spain;

²Plant-Soil-Interactions, Institute for Sustainability Sciences, Agroscope, Reckenholzstrasse 191, 8046 Zürich, Switzerland; ³Institute of Plant Sciences, University of Bern, Altenbergrain 21,

3013 Bern, Switzerland; ⁴Department of Environmental Sciences, University of Basel, Bernoullistrasse 32, 4056 Basel, Switzerland; ⁵Soil Microbiology and Symbiotic Systems Department,

Estación Experimental del Zaidín (EEZ-CSIC), Profesor Albareda 1, Granada 18008 Spain; ⁶Department of Evolutionary Biology and Environmental Studies, University of Zurich,

Winterthurerstrasse 190, 8057 Zürich, Switzerland; ⁷Plant-Microbe-Interactions, Department of Biology, Utrecht University, 3508TB Utrecht, the Netherlands

Summary

Author for correspondence:

José Ignacio Querejeta

Email: querejeta@cebas.csic.es

Received: 23 April 2021

Accepted: 23 July 2021

New Phytologist (2021) **232**: 1399–1413

doi: 10.1111/nph.17661

Key words: dissolved nitrogen, dissolved organic carbon, extracellular hydrolytic soil enzymes, fungal functional guilds, Gadgil effect, mixed arbuscular/ectomycorrhizal (AM/EM) ecosystems, mycorrhizal nutrient economy.

- The aboveground impacts of climate change receive extensive research attention, but climate change could also alter belowground processes such as the delicate balance between free-living fungal decomposers and nutrient-scavenging mycorrhizal fungi that can inhibit decomposition through a mechanism called the Gadgil effect.
- We investigated how climate change-induced reductions in plant survival, photosynthesis and productivity alter soil fungal community composition in a mixed arbuscular/ectomycorrhizal (AM/EM) semiarid shrubland exposed to experimental warming (W) and/or rainfall reduction (RR). We hypothesised that increased EM host plant mortality under a warmer and drier climate might decrease ectomycorrhizal fungal (EMF) abundance, thereby favouring the proliferation and activity of fungal saprotrophs.
- The relative abundance of EMF sequences decreased by 57.5% under W+RR, which was accompanied by reductions in the activity of hydrolytic enzymes involved in the acquisition of organic-bound nutrients by EMF and their host plants. W+RR thereby created an enhanced potential for soil organic matter (SOM) breakdown and nitrogen mineralisation by decomposers, as revealed by 127–190% increases in dissolved organic carbon and nitrogen, respectively, and decreasing SOM content in soil.
- Climate aridification impacts on vegetation can cascade belowground through shifts in fungal guild structure that alter ecosystem biogeochemistry and accelerate SOM decomposition by reducing the Gadgil effect.

Introduction

Climate change models predict large increases in temperature and atmospheric vapour pressure deficit in the Mediterranean region as a consequence of anthropogenic global warming, which will be accompanied by reductions in the amount and frequency of precipitation (Guiot & Cramer, 2016). Projected climate aridification trends will therefore increase heat and drought stress for plants and their symbiotic mycorrhizal fungi in many dryland areas, leading to reductions in plant survival and aboveground primary productivity that could also alter belowground processes (León-Sánchez *et al.*, 2018, 2020).

Plants and their mycorrhizal fungi may compete with decomposers for soil N and other nutrients, especially in low-fertility ecosystems with poor litter quality (Lindahl *et al.*, 2005; Bödeker *et al.*, 2016; Fernandez *et al.*, 2020). Ectomycorrhizal fungi (EMF) produce N-degrading enzymes that allow them access to organic-bound N sources (Read & Perez-Moreno, 2003; Averill *et al.*, 2014; Averill & Hawkes, 2016; Tedersoo & Bahram, 2019). Decomposition of litter and soil organic matter (SOM) is often constrained by low nitrogen availability to free-living microbial decomposers (Schimel & Bennett, 2004). EMF can outcompete saprotrophic fungi for organic-bound nutrients present in litter and SOM thanks to high carbon allocation from host plants, which can lead to slowed or suppressed degradation of litter and SOM, a mechanism known as the ‘Gadgil effect’ (Gadgil & Gadgil, 1971). According to the N-mining hypothesis

*These authors contributed equally to this work.

(Orwin *et al.*, 2011), EMF selectively forage for organic-bound nutrients and hydrolyse or oxidise SOM to obtain small organic N-rich compounds, leaving behind a nutrient-poor and C-enriched substrate (Perez-Moreno & Read, 2000; Pritsch & Garbaye, 2011). This may result in nutrient limitation of free-living saprotrophs, thereby inhibiting decomposition of SOM and enhancing soil carbon storage in low-fertility ecosystems (Clemmensen *et al.*, 2013; Zak *et al.*, 2019). EMF mycelia further contribute to the formation of mineral-stabilised SOM through hyphal exudation of mineral surface reactive metabolites (Wang *et al.*, 2017; Frey, 2019). Arbuscular mycorrhizal fungi (AMF) have less complex enzymatic capabilities than EMF, which limit their ability to access and exploit organic nutrient sources (Averill & Hawkes, 2016). However, AMF can also inhibit litter decomposition by saprotrophs and might contribute to the Gadgil effect in nutrient-poor habitats (Leifheit *et al.*, 2015).

Global changes that alter the competitive interactions between mycorrhizal fungi and microbial decomposers could influence soil carbon storage at regional to global scales (Soudzilovskaia *et al.*, 2019). The potential impacts of climate aridification on the competitive balance between soil fungal guilds and the Gadgil effect have received limited research attention, despite the widespread occurrence of climate change-induced changes in soil fungal community structure and functionality (Compant *et al.*, 2010; Yuste *et al.*, 2011; Bastida *et al.*, 2017). The abundance and diversity of EMF in dryland ecosystems often decrease with climate warming and drying (Swaty *et al.*, 1998, 2004; Querejeta *et al.*, 2009). This may be due to reduced carbon allocation by climatically stressed host plants with poorer photosynthesis and demand for nutrients, and/or to low tolerance of some EMF to soil desiccation and heat stress (Coleman *et al.*, 1989; Nickel *et al.*, 2018). Even more importantly, increased EM host plant mortality with hotter droughts could drastically reduce EMF abundance and diversity in drylands under a climate aridification scenario (Mueller *et al.*, 2005; León-Sánchez *et al.*, 2018).

Studies focusing on vegetation types that associate with both EMF and AMF may enhance our understanding of the extent to which mycorrhizal fungi contribute to SOM dynamics and ecosystem nutrient economy (Phillips *et al.*, 2013). Mixed EM/AM shrublands dominated by shrubs of the *Cistaceae* family are endemic-rich communities that occupy vast areas of the drier parts of the Mediterranean region (Comandini *et al.*, 2006; Leonardi *et al.*, 2018; Marqués-Gálvez *et al.*, 2020). Shrublands allow easier experimental manipulation of temperature and rainfall than forests due to smaller plant size and, therefore, provide convenient model systems for assessing the impacts of simulated climate warming and drying on vegetation and soil fungal communities (León-Sánchez *et al.*, 2018, 2020). Manipulative experiments in shrublands offer an untapped potential for assessing climate-induced changes in the strength of the Gadgil effect in intact soil, as temperature and rainfall modification could induce changes in fungal guild dominance without the need for direct manipulation of the belowground compartment (Bennett & Classen, 2020). Moreover, native shrubs growing on low-fertility dryland soils show high foliar carbon-to-nutrient ratios and poor litter quality linked to high nutrient resorption efficiencies before

foliar senescence (Prieto *et al.*, 2019; Prieto & Querejeta, 2020), which should enhance the strength of the Gadgil effect through intense competition for scarce nutrients between fungal guilds.

Here, we propose and experimentally test a conceptual model of the impacts of climate aridification on soil fungi and SOM dynamics in low-fertility drylands (Fig. 1). We tested our model in mixed EM/AM semiarid shrubland communities that were exposed to 4 yr of experimental climate manipulation. In a recent companion paper we reported the strong negative impacts of warming and rainfall reduction (W+RR) on the native shrubs, including large increases in heat-related and drought-related mortality and decreases in the photosynthesis and productivity of the surviving individuals (León-Sánchez *et al.*, 2020). In particular, the two main EM host shrub species (*Helianthemum syriacum*, *Helianthemum squamatum*) present in the experimental plots exhibited 68–72% mortality over 4 yr in the W+RR treatment, along with 28–47% reductions in photosynthesis and 47–56% reductions in shoot biomass growth relative to control plants. Here, we test the following hypotheses: (1) Higher mortality and lower photosynthesis of EM host plants will decrease EMF abundance under W+RR. (2) Decreased carbon availability for allocation to EMF in climatically stressed survivor host plants will reduce the EMF ability to produce metabolically expensive enzymes needed for nutrient mining of SOM under W+RR. (3) Climate aridification will thereby alleviate the nutrient limitation of free-living fungal decomposers through competitive release from EMF and their host plants under W+RR. (4) Reduced strength of the Gadgil effect under W+RR will stimulate the proliferation and activity of fungal decomposers and will thereby enhance nitrogen mineralisation and SOM decomposition in these nutrient-poor soils. (5) By contrast with EMF, AMF abundance will remain largely unaffected because some AM host shrubs showed high survival rates under W+RR (75–100% survival in *Gypsophila struthium*, *Teucrium turredanum*; León-Sánchez *et al.*, 2020), which should allow them to continue supporting their AMF symbionts.

Materials and Methods

Study site, experimental design and soil sampling

This study was conducted near Sorbas in Southeastern Spain (37°05'N–2°04'W; 400 m asl). The climate is semiarid Mediterranean, with mild winters and dry, hot summers. Mean annual temperature is 17°C and rainfall is 275 mm occurring mostly in autumn and spring. Soils have high gypsum content (>50%), high pH (>7) and low organic carbon content and fertility (Supporting Information Table S1). Vegetation is a mixed EM/AM shrubland dominated by the perennial tussock grass *Stipa tenacissima* and several woody shrub species.

In May 2011 we started a randomised factorial experiment in the field with two experimental factors: warming (W) and rainfall reduction (RR). To simulate the predictions for the second half of the 21st century in the Mediterranean region (Giorgi & Lionello, 2008), open-top chambers (OTCs) were used to achieve temperature elevation. OTCs are hexagonal chambers,

Climate warming and drying in mixed EM/AM semiarid shrublands

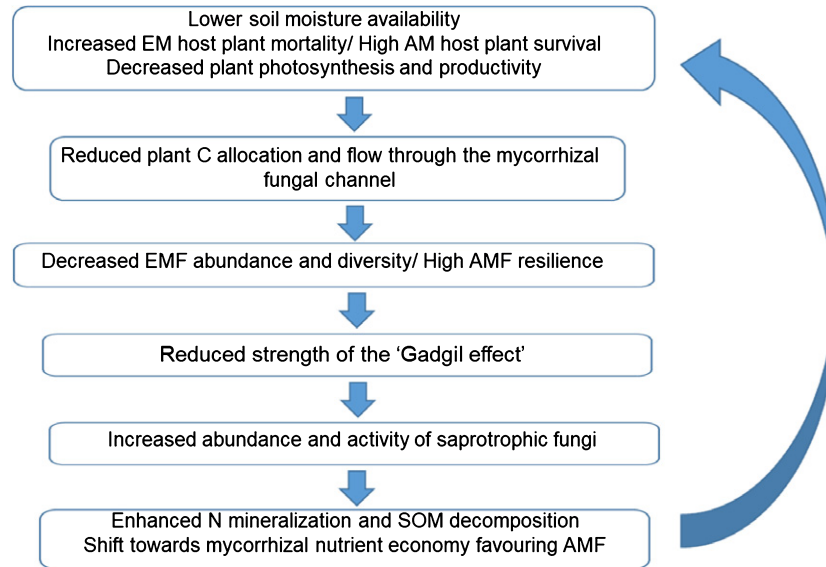


Fig. 1 Conceptual model hypothesising that high ectomycorrhizal (EM) host plant mortality and decreased abundance of ectomycorrhizal fungi (EMF) under simulated climate warming and rainfall reduction (W+RR) may reduce the magnitude of the Gadgil effect and, therefore, may lead to enhanced soil nitrogen mineralisation and organic matter (SOM) decomposition by fungal saprotrophs. The conceptual model is based on previous findings by León-Sánchez *et al.* (2020) showing high heat-related and drought stress-related mortality (68–72%) of EM shrub species (*Helianthemum syriacum*, *Helianthemum squamatum*) along with decreased photosynthesis and productivity of the surviving EM plants in the W+RR treatment. By contrast, some of the arbuscular mycorrhizal (AM) shrub species present in the same experimental plots (*Gypsophila struthium*, *Teucrium turredanum*) exhibited markedly high survival rates under W+RR (75–100%) despite decreased photosynthesis and productivity, which should enable them to continue supporting their arbuscular mycorrhizal fungal (AMF) symbionts under hotter and drier climatic conditions. Enhanced SOM mineralisation by fungal decomposers combined with reduced vegetation photosynthesis, productivity and litter inputs to soil in W+RR could trigger a feedback loop that leads to progressive decline of SOM content and ecosystem nutrient and water retention capacity in low-fertility EM/AM semiarid shrublands exposed to climate aridification.

with sloping slides of $40 \times 50 \times 32$ cm (Fig. S1). They are made of methacrylate, which transmits *c.* 92% of visible light, has a reflection of incoming radiation of 4%, and passes on 85% of incoming energy (Decorplax SL, Spain). OTCs were suspended *c.* 3 cm above the ground by metal frames allowing free air circulation and exchange with the surrounding environment to minimise undesirable experimental artefacts (Hollister & Weber, 2000). Upon installation in the field, the vertical height of the OTCs was 40 cm. Passive rainout shelters were used to simulate rainfall reduction, which is achieved by suspending transparent methacrylate troughs covering *c.* 30% of the plot area over an aluminium frame above the plots (height 130 cm, width 100×100 cm; Fig. S1). Intercepted rainwater (30%) is diverted through pipes, collected in tanks and removed. Both OTCs and rainout shelters were installed over the same plots to achieve the combined warming plus rainfall reduction effect (W+RR). Climate treatments were randomly assigned to plots: 10 plots with OTCs only (W), 10 with rainout shelters only (RR) and 11 combining OTCs with rainout shelters (W+RR), along with 32 control plots (of which 19 were randomly selected for this study).

Air temperature/relative humidity and topsoil (0–5 cm) temperature and moisture content were monitored using replicated automated sensors (HOBO[®]U23 Pro v.2 Temp/RH, TMC20-HD sensors; Onset Corp., Pocasset, MA, USA; EC-5 moisture sensors; Decagon Devices Inc., Pullman, WA, USA, respectively). OTCs increased mean annual air temperature by *c.* 2°C in the W

and W+RR plots, relative to control conditions, with larger increments during warm periods (4–5°C during hot days in summer) than during cold periods (*c.* 1°C). Topsoil mean annual temperature was 2.2°C higher and topsoil moisture content was 16% lower in the warmed plots (W and W+RR) than in control plots. Rainout shelters reduced topsoil moisture content by 14% but did not alter air or soil temperatures (León-Sánchez *et al.*, 2020).

The dominant shrub species in the experimental plots were *Helianthemum syriacum* (Cistaceae, 30.7% plant cover), *Helianthemum squamatum* (Cistaceae, 2.4%), *Gypsophila struthium* (Caryophyllaceae, 20.6%), *Teucrium turredanum* (Lamiaceae, 8.6%), *Santolina viscosa* (Asteraceae, 11.4%) and *Coris hispanica* (Primulaceae, 2.7%). Other perennial woody shrubs and annuals were also present (23.6% cover in total). The two *Helianthemum* species are primarily EM but can also establish symbiotic associations with AMF, whereas the remaining shrub and annual species are strictly AM (Brundrett, 2009).

Extensive root sampling to assess mycorrhizal root colonisation and fungal identity in each shrub species would have implied destructive root excavation and severe disruption of our experimental system. Moreover, root species identification was hampered by the coexistence of several shrub species growing together within the same vegetation patches, which leads to root overlap and intermingling between neighbour shrubs. We focused instead on the fungal community present in rhizosphere soil

under shrubs. At 4 yr after the start of the experiment (May 2015), 50 rhizosphere soil samples (0–15 cm depth) were collected with a hand auger corer (5 cm diameter) under the canopy of *H. syriacum* (27) or *G. struthium* (23) shrubs. Here, 19 control plots were randomly selected for soil sampling, along with 10 W plots, 10 RR plots and 11 W+RR plots. The 50 rhizosphere samples (one soil core taken per experimental plot) were transported to the laboratory on ice and sieved through 2 mm. A soil subsample was stored in sealed plastic bags at -80°C until DNA extraction, whereas the remaining soil was stored at 4°C for biochemical analyses.

Soil DNA extractions

Total genomic DNA was extracted from 300 mg of each rhizosphere soil sample, using the FastDNA spin kit for soil (MP Biomedicals, Santa Ana, CA, USA) and following the manufacturer's protocol. Extracted DNA was checked in 1% agarose gels run in $0.5\times$ Tris–acetate–EDTA (TAE) buffer (100 V, 15 min) to assess the quality of the extractions and the yield was quantified using a Quant-iT PicoGreen dsDNA Assay Kit (Invitrogen, Eugene, OR, USA) on a Varian Cary Eclipse fluorescence spectrometer (Agilent Technologies, Santa Clara, CA, USA).

ITS PCR, library preparation and sequencing

We analysed the rhizosphere fungal communities using a bar-coded high-throughput sequencing approach similar to McGuire *et al.* (2013). The first internal transcribed spacer region (ITS1) was amplified by PCR using the universal fungal primers ITS1F (CTTGGTCATTTAGAGGAAGTAA; Gardes & Bruns, 1993) and ITS2 (GCTGCGTTCTTCATCGATGC; White *et al.*, 1990). We utilised a dual barcoding approach with 8-bp error-correcting unique barcodes on both primers (5'-barcode–primer-3'; Method S1 lists the sample-to-barcode assignments).

All DNA samples were amplified in triplicate PCR reactions of a total volume of 25 μl , consisting of 12 μl of water, 10 μl $2.5\times$ 5 Prime Hot Master Mix, 1 μl each of the forward and reverse primers (5 μM final concentration), and 1.0 ng genomic DNA as template. Thermal cycling was performed on an iCycler PCR Instrument (Bio-Rad) using the following conditions: an initial denaturation step at 94°C for 3 min, with amplification proceeding for 35 cycles at 94°C for 45 s, 50°C for 60 s, and 72°C for 90 s; a final extension of 10 min at 72°C . The products of the triplicate PCR reactions were pooled, confirmed on a 1% agarose gel (Sigma-Aldrich, USA) for absence of contamination in negative control samples, and purified from PCR reagents using the 'PCR reaction clean-up' kit (Macherey-Nagel, Düren, Germany) following the manufacturer's instructions. Amplicon concentrations were quantified on a Varian Eclipse Fluorescence plate reader (Agilent Technologies, Santa Clara, CA, USA) using Quant-iT PicoGreen dsDNA Assay Kit (Invitrogen) and Herring Sperm DNA (Invitrogen) as standard solution. Amplicons from all samples were pooled in equimolar concentrations, purified using Agencourt AMPure XP beads (Beckman Coulter, Krefeld, Germany). Library preparation including ligation of Illumina

adapters and sequencing on the MiSeq Instrument (Illumina, San Diego, CA, USA; 2×300 bp, v.3 Sequencing kit) was performed at the Functional Genomics Center Zurich. We typically sequenced various experiments in one MiSeq run, which was deposited with an earlier study (Hartman *et al.*, 2018). The raw sequencing data are available from the European Nucleotide Archive (<http://www.ebi.ac.uk/ena>) with the sample ID SAMEA4711908 under the study accession PRJEB21595. The sequences of this study can be extracted from the raw data based on the barcodes and primers indicated in Methods S1.

Bioinformatics

Raw reads were processed using the bioinformatics pipeline documented in Methods S2. Reads were prequality filtered (max. 1 N, min. length 100 bp) and trimmed at the 3'-end to 280 bp using PRINSEQ (Schmieder & Edwards, 2011) and then merged with FLASH (Magoč & Salzberg, 2011). Sequences were demultiplexed using CUTADAPT (Martin, 2011) and were quality-filtered with PRINSEQ (30–70% GC, min. quality 20, no N allowed). For operational taxonomic unit (OTU) delineation the ITS sequences were trimmed to the fixed length of 220 bp, sorted by abundance, de-replicated, and clustered to OTUs ($\geq 97\%$, singletons removed) with UPARSE (Edgar, 2013). Chimeric sequences were screened using UCHIME (Edgar *et al.*, 2011) against the UNITE database (Abarenkov *et al.*, 2010) and removed. Taxonomy assignment was performed using the UNITE database (v.7.0) with the RDP classifier as implemented in QIIME (Caporaso *et al.*, 2010). Fungal OTUs were classified into functional guilds using FUNGUILD database v.1.1 (Nguyen *et al.*, 2016).

Fungal community analysis in R

To avoid bias by differences in sequencing effort we normalised the data by rarefying the samples to 2187 sequences. To assess whether the fungal community structure was affected by the climate manipulation factors (warming, rainfall reduction and their interaction), a permutational multivariate analysis of variance (PERMANOVA) was performed with the *adonis* function in the VEGAN package for R (Oksanen *et al.*, 2016) using Hellinger-based distances as a measure of dissimilarity and 999 permutations. A redundancy analysis ordination (RDA) using Hellinger-based distances was performed to visualise differences in fungal community structure among climate treatments (*rda* function, VEGAN package in R). The alpha diversity indices (OTU richness, Shannon-Weaver and Pielou evenness indexes) were calculated for the entire soil fungal community and for each of the main fungal functional guilds separately (*specnumber* and *diversity* functions, VEGAN package in R). All microbiota analysis were performed in R (v3.6.1; R Core Team, 2019; Methods S3).

Rhizosphere soil chemical and biochemical analyses

Free soil water content was measured gravimetrically at low temperature (40°C , 72 h) to avoid release of gypsum crystallisation

water. Total organic carbon (TOC) and total nitrogen contents were measured using an Elemental Analyser (C/N FLASH EA 1112 Series Leco-Truspec). Soil organic matter (SOM) contains *c.* 58% C; therefore, a factor of 1.72 can be used to convert TOC to SOM (Guo & Gifford, 2002). Dissolved organic carbon (DOC) and dissolved nitrogen (DN, including inorganic and organic N) were measured in soil water extracts (1 : 5, w/v) with a Multi N/C 3100 Analyser (Analytik Jena, Jena, Germany). Soil microbial decomposers convert polymeric SOM to DOC, which is the main rate-limiting step in SOM decomposition. DOC and DN contents in soil and therefore provide an indication of the SOM decomposition and N mineralisation processes, respectively (Allison *et al.*, 2010). DOC and DN values were normalised by soil TOC content and log-transformed before statistical analyses. The extractable C of the humic compounds in soil (humic and fulvic acids, which are the stable and recalcitrant fractions of SOM) was determined in the alkaline sodium pyrophosphate extract by oxidation with potassium dichromate in an acid medium (H₂SO₄) and measured spectrophotometrically (Stevenson, 1985). The soil electrical conductivity (EC) and pH were measured in the aqueous extract (1 : 5, w/v), using a conductance meter and a pH meter (GLP 31 and GLP 21, Crison Instruments, Hach Lange Spain).

Extracellular nutrient-acquiring enzyme activities involved in the acquisition of organic-bound N and P by plants, EMF and other soil microorganisms were measured in freshly collected soil samples. Urease activity was determined as the ammonium released in the hydrolytic reaction using urea as substrate (Kandeler *et al.*, 1999). Glycine-aminopeptidase (GAP) activity was determined by spectrophotometry measuring the product of the protein degradation (*p*-nitroaniline) in the soil extract. Alkaline phosphomonoesterase activity was determined by measuring the *p*-nitrophenol released in the hydrolytic reaction by colorimetry (Tabatabai & Bremner, 1969) in a UV-vis spectrophotometer (Helios Alpha, Thermo, Cambridge, UK). Extracellular enzyme activities were normalised by the microbial biomass content in soil samples (see below) to calculate specific enzyme activities, which indicate the proportional allocation of microbes into enzyme synthesis (Hacker *et al.*, 2015; Zuo *et al.*, 2018).

Dehydrogenase enzyme activity was determined as the reduction of *p*-iodonitrotetrazolium chloride to *p*-iodonitrotetrazolium formazan (INTF) by measuring the absorbance of INTF in a spectrophotometer (Trevors *et al.*, 1982). Dehydrogenase activity provides an index of the metabolic activity of living heterotrophic soil microbes, as it is linked to intact and viable microbial cells only and plays a key role in intracellular oxidative degradation processes (e.g. dehydrogenation and oxidation of SOM; Ross, 1971; Quilchano & Marañón, 2002).

Microbial heterotrophic respiration was measured by placing 1 g of soil in a sealed flask, moistened to 60% of the soil water holding capacity and then incubated for 1 month at 28°C (García *et al.*, 1994). The CO₂ evolved was measured weekly using a gas chromatograph (GC/FID, AutoSys-tem XL Gas Chromatograph; Perkin-Elmer, Norwalk, CT, USA), and respiration was calculated as $\mu\text{g C-CO}_2 \text{ g}^{-1} \text{ soil d}^{-1}$.

For evaluation of the total microbial biomass content in soil (fungi plus bacteria), microbial phospholipid fatty acids (PLFAs) were extracted from 6 g of soil using a chloroform-methanol extraction, and fractionated and quantified using the procedure described by Bardgett *et al.* (1996). Phospholipids were transformed by alkaline methanolysis into fatty acid methyl esters (FAMES), which were quantified by a gas chromatograph (TRACE GC Ultra; Perkin-Elmer). More specifically, the PLFA 18:2 ω 6, 9 was used to assess the fungal biomass content in soil samples (Frostegard & Baath, 1996).

Statistical analyses

Two-way ANOVAs were used to assess the impacts of the two experimental climate factors (W and RR) and their interaction (W \times RR) on the relative sequence abundances of fungal guilds and soil parameters. Post-hoc tests (LSD pairwise means comparisons adjusted for multiple comparisons) were used to assess significant differences between climate treatments. Pearson correlation, stepwise regression and principal component analyses (PCA) were used to examine the relationships between fungal guild relative sequence abundances and soil properties. Non-normal variables were log-, square root or arcsin transformed before statistical analyses, conducted using SPSS 27.0 software (SPSS Inc., Chicago, IL, USA).

Results

Overall fungal community structure

The number of fungal sequences per soil sample ranged from 2187 to 24 178. Rarefaction curves revealed that the sequencing effort was sufficient to capture the majority of the fungal diversity present (Fig. S2). Sequencing of the fungal ITS region yielded a total of 827 439 high-quality sequences, which were clustered into 2092 fungal OTUs. Of these, 851 OTUs corresponded to unidentified fungi in UNITE. The soil fungal community was dominated by Ascomycota (65.6%), as usually encountered in drylands (Fig. S3). We were able to assign 1181 OTUs to functional guilds according to FUNGuild, of which the majority had 'probable' or 'highly probable' guild status. Here, 60 additional OTUs with no results in FUNGuild were manually assigned to guilds based on careful revision of the fungal literature (Methods S4). Among the resulting 1241 OTUs assigned to guilds, 367 OTUs were classified as EMF, 544 as saprotrophs, 111 as AMF, 122 as plant pathogens, 27 as lichenised fungi, 29 as animal pathogens, 26 as plant endophytes, 15 as fungal parasites.

Impact of experimental climate manipulation on rhizosphere fungal communities

PERMANOVA analysis of the rhizosphere fungal community through Hellinger-based OTU distance metrics revealed significant impacts of the experimental warming factor ($P=0.010$), the rainfall reduction factor ($P=0.032$) and their interaction (marginal effect, $P=0.084$) on fungal community structure

(Table S2; Fig. S4). Nearly identical results were obtained when using rarefied or nonrarefied data in the PERMANOVA (Table S2). Mean fungal OTU richness per soil sample was marginally reduced with warming ($P=0.078$; Table S3).

The relative abundance of EMF sequences in rhizosphere soil was decreased by both experimental warming ($P=0.027$; Table S4) and rainfall reduction ($P=0.025$). EMF sequence abundance was highest in the control treatment and lowest under W+RR (57.5% reduction relative to control; Figs 2, 3). The average richness of EMF OTUs per soil sample was also decreased by warming ($P=0.037$; Table S3). The relative abundance of EMF basidiomycetes with medium-distance or long-distance hyphal exploration types (*Cortinari*, *Scleroderma*, *Thelephoraceae*) was decreased by rainfall reduction ($P=0.019$), and was lowest under W+RR (Fig. S5).

The relative abundance of saprotrophic fungal sequences was increased by experimental warming ($P=0.014$; Table S4) and marginally by rainfall reduction ($P=0.077$). Saprotroph sequence abundance was lowest in the control treatment and highest under W+RR (39.9% increase relative to control, Figs 2, 3, S5, S6). However, the diversity (Shannon) and evenness (Pielou) of the saprotrophic fungal guild decreased with warming ($P=0.019$ and $P=0.025$, respectively; Table S3), revealing increased dominance by fewer saprotrophic taxa in the W and W+RR treatments (e.g. *Filobasidium*, *Davidiella*, *Gliomastix* sp.).

Analysis of the raw fungal sequence abundances in rhizosphere soil (Fig. S7) further confirmed the patterns observed for relative abundance data: raw EMF sequence abundance decreased with both warming ($P=0.016$) and rainfall reduction ($P=0.005$), whereas the raw sequence abundance of saprotrophic fungi increased with warming ($P=0.030$).

Total fungal biomass content in soil was similar between the control and W+RR treatments (Tables S5, S6), so the drastic

change in guilds raw and relative abundances observed under W+RR necessarily translates into decreased EMF biomass coupled with increased biomass of fungal saprotrophs in absolute terms, compared with the control. Interestingly, higher EM plant mortality was linked to lower EMF abundance across climate treatments ($r=-0.810$, $P=0.015$). The mean mortality rate of EM host plant species (*H. syriacum*, *H. squamatum*) explained 60% of the variation in EMF abundance across climate treatments. The abundance of EMF sequences also decreased with decreasing EM host plant photosynthesis ($r=0.702$, $P=0.052$) and foliar biomass production (0.758, $P=0.029$).

The relative abundances of sequences belonging to other fungal guilds were comparatively low across climate treatments: 8.4% plant pathogens; 1.4% AMF; 0.9% plant endophytes; 0.8% lichenised fungi; 0.4% fungal parasites; 0.3% animal pathogens (Fig. 2). Plant pathogens abundance was increased by warming ($P=0.025$), whereas animal pathogens abundance was marginally enhanced by rainfall reduction ($P=0.071$; Table S4). The relative abundance of AMF sequences in rhizosphere soil was highest (2.24%) in the W+RR treatment (significant W \times RR interaction; $P=0.002$; Table S4; Fig. 2). The AMF community was dominated by Glomeraceae across treatments (Fig. S8).

Impact of the climate manipulation treatments on rhizosphere soil

Topsoil water content was very low (<2%) in all climate treatments at time of sampling (Fig. S9). Urease, GAP and alkaline phosphomonoesterase enzymatic activities were 56–46% lower under W+RR than in the control treatment (Fig. S10), which suggests a decreased ability of EMF and their host plants to hydrolyse and access organic-bound N and P sources in soil

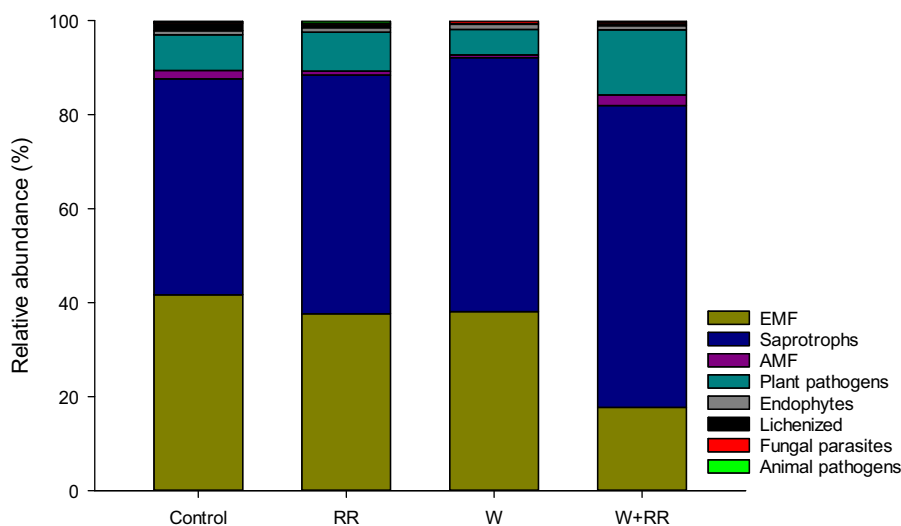


Fig. 2 Mean relative abundance of fungal operational taxonomic units (OTUs) belonging to eight major functional guilds in rhizosphere soil in the different climate treatments. Climate treatments are Control, rainfall reduction (RR), Warming (W) and Warming plus rainfall reduction (W+RR). $n = 10$ –19 soil samples per treatment. Relative abundances were calculated relative to the total number of fungal OTUs that could be assigned to functional guilds (1241 OTUs, or c. 60% of the total number of OTUs detected). The remaining 851 OTUs corresponding to unidentified fungi in UNITE (c. 40% of the total) could not be assigned to functional guilds and are not included in this graph. AMF, arbuscular mycorrhizal fungi; EMF, ectomycorrhizal fungi.

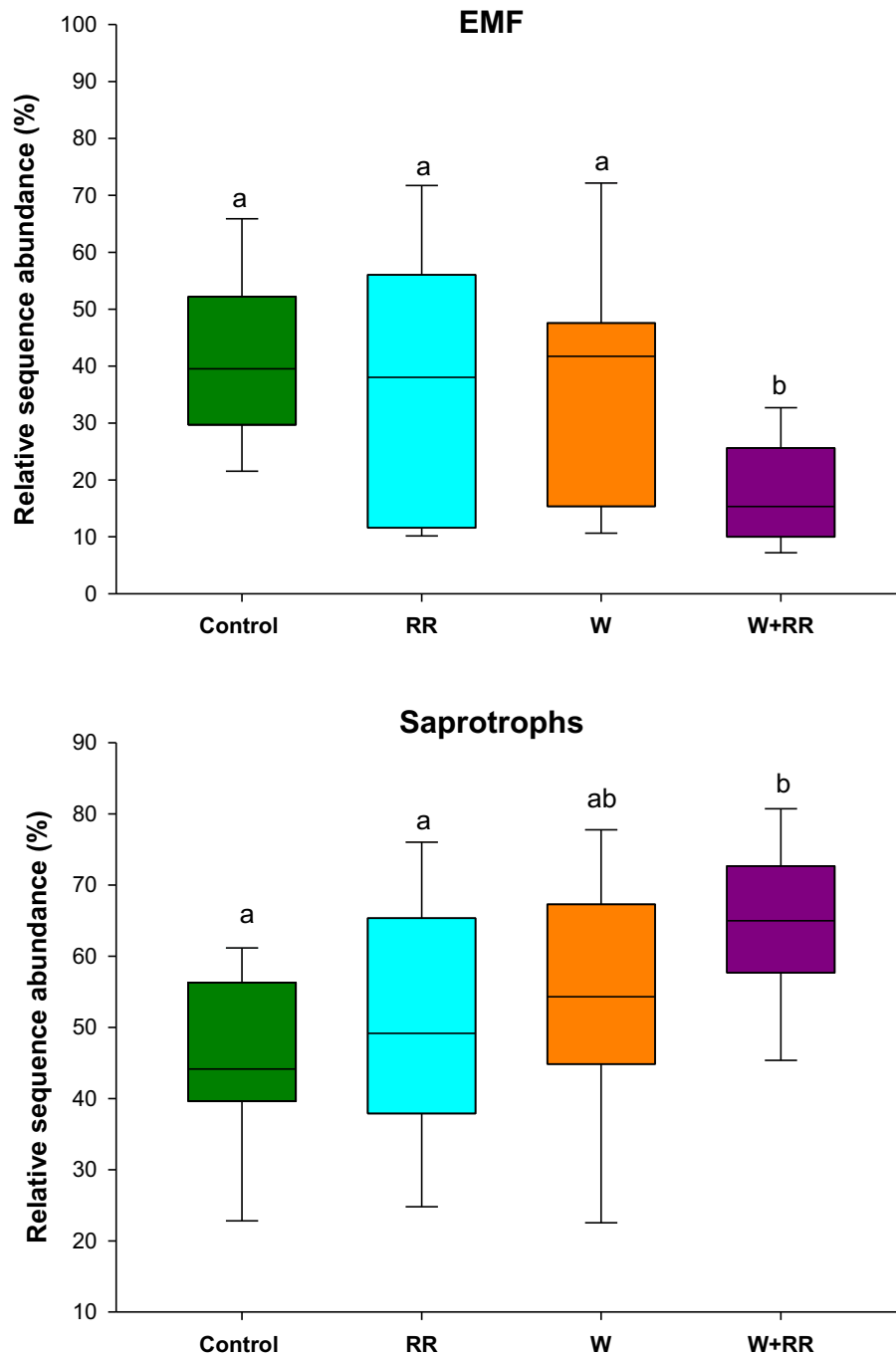


Fig. 3 Relative abundance of ectomycorrhizal (EMF, upper panel) and saprotrophic (lower panel) fungal sequences in rhizosphere soil (0–15 cm depth) in the four climate treatments. Means and standard errors ($n = 10–19$) are shown for each climate treatment (Control; RR, rainfall reduction; W, warming; W+RR, warming plus rainfall reduction). Different letters indicate significant differences among climate treatments according to LSD post-hoc tests. Relative abundances were calculated relative to the total number of fungal OTUs that could be assigned to functional guilds (1241 OTUs, or c. 60% of the total number of OTUs detected).

under warmer and drier climate conditions. Phosphatase and GAP activities correlated positively with soil moisture content across soil samples ($r = 0.471$, $P < 0.001$; $r = 280$, $P = 0.051$, respectively).

The combination of warming and rainfall reduction led to a nearly two-fold increase of DOC and three-fold increase of DN contents in soil (Fig. 4), suggesting enhanced SOM

decomposition and N mineralisation by free-living saprotrophic microbes under W+RR. Moreover, the abundance of humic substances in soil was marginally decreased by warming ($P = 0.071$; Fig. S11), which further suggests an enhanced decomposition of recalcitrant, stabilised humic compounds. Soil DOC content correlated negatively with soil water content ($r = -0.290$, $P = 0.043$), whereas DN content was unaffected by soil moisture.

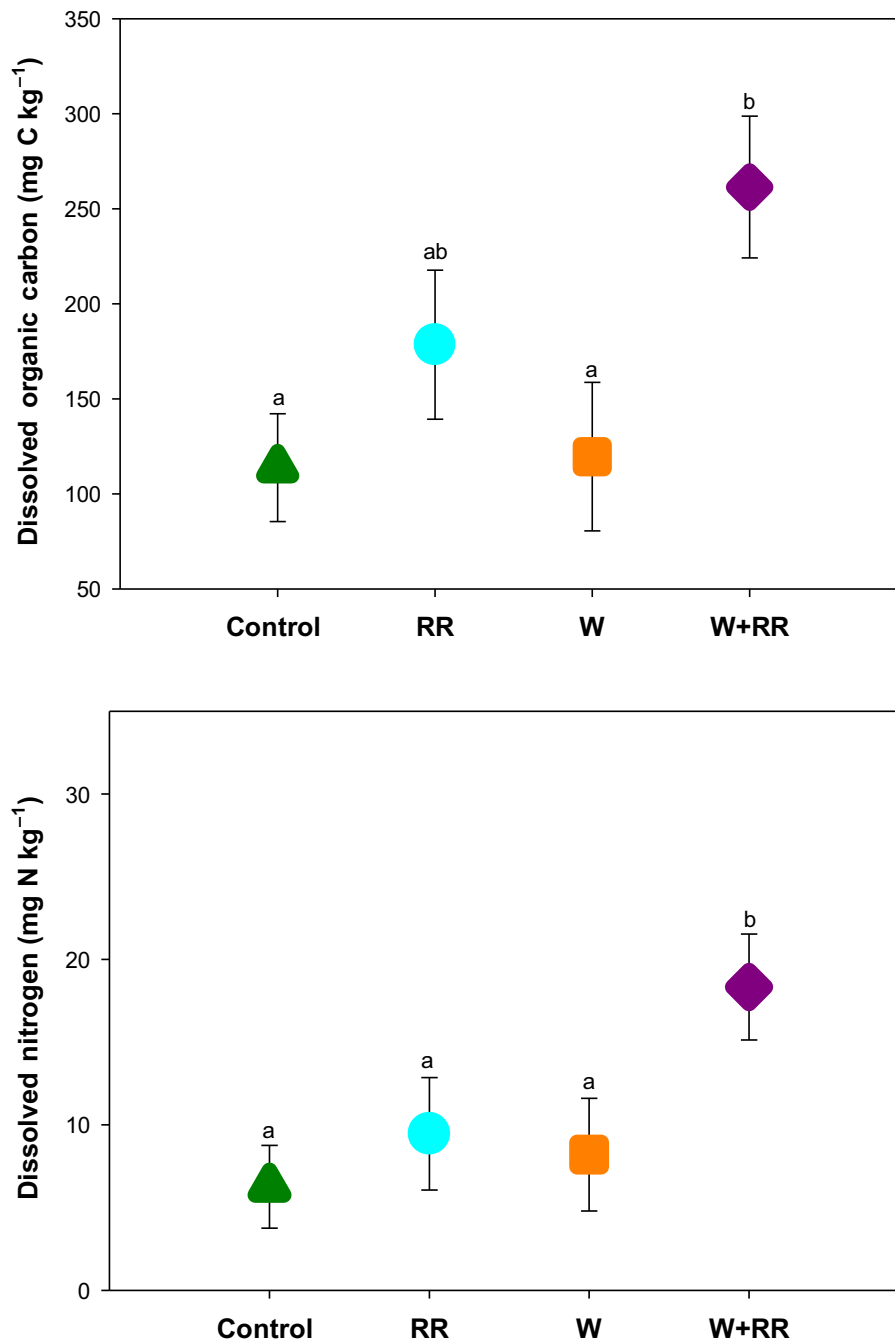


Fig. 4 Dissolved organic carbon (DOC, upper panel) and dissolved nitrogen (DN, lower panel) contents in soil in the different climate treatments (Control; W, warming; RR, rainfall reduction; W+RR, warming plus rainfall reduction). Means and standard errors are shown ($n = 10\text{--}19$). Different letters indicate significant differences among climate treatments according to LSD post-hoc tests.

Microbial biomass content in soil (fungi + bacteria) was highest under W+RR (Tables S5, S6). Microbial heterotrophic respiration rate and dehydrogenase activity were on average 14–15% and 14–23% higher, respectively, in all the climate change treatments than in the control treatment, although differences were not statistically significant due to large heterogeneity among plots (Tables S5, S6). A PCA analysis including four key soil variables linked to SOM decomposition (DOC/DN contents, dehydrogenase activity, microbial heterotrophic respiration) yielded a single PCA axis encompassing over 70% of the total variance, and with

all four variables loading heavily on this axis (Table S7). Average scores along PCAaxis1 were lowest in the control treatment and highest under W+RR (post-hoc LSD test, $P < 0.05$).

Relationships between main fungal guild abundances and soil parameters

The relative abundance of EMF sequences was positively associated with urease activity, a nutrient-acquiring extracellular enzyme involved in the hydrolysis of organic-bound nitrogen

(Fig. 5). EMF abundance was also positively associated with the humic compounds content in soil (Fig. 5). By contrast, EMF abundance was strongly negatively associated with soil DOC and DN contents, heterotrophic microbial respiration rate and dehydrogenase activity (Figs 5, S12). The scores of rhizosphere soil samples along PCAaxis1 decreased with increasing abundance of EMF sequences ($r = -0.479$, $P < 0.001$; Fig. S13), which overall supports inhibition or suppression of SOM decomposition by EMF. The relative abundance of EMF basidiomycetes with medium-distance and long-distance hyphal exploration types (*Scleroderma*, *Cortinarius*, *Thelephoraceae*) correlated negatively with soil DOC and DN contents, but positively with urease activity and humic compounds content in soil (Fig. 5).

The relative abundance of saprotrophic fungal sequences correlated positively with soil DN and DOC contents, dehydrogenase activity (Fig. 5) and soil scores along PCAaxis1 ($r = 0.375$, $P = 0.007$), suggesting stimulation of both SOM decomposition and N mineralisation with increasing saprotrophs abundance. Moreover, the abundance of saprotrophic fungi was negatively associated with humic compounds content in soil (Fig. 5).

Stepwise regression and structural equation models (SEM) revealed that soil DOC content in soil samples was best predicted

by the abundance of EMF with medium-distance and long-distance exploration types, while soil water content and AMF abundance explained additional variance. EMF abundance was the single predictor of DN content (Table S8; Fig. S14) across soil samples.

Impacts of simulated climate warming and drying on the temporal evolution of SOM content

Topsoil SOM content (0–15 cm) decreased by 29% in the W+RR treatment between 2015 and 2020, which differed significantly from the increase in SOM content observed in the Control treatment ($P = 0.014$; Fig. 6). This finding suggests an enhanced rate of SOM decomposition by saprotrophs linked to the sharp reduction in EMF abundance observed under W+RR. Across plots, lower relative abundance of EMF with medium-distance and long-distance hyphal exploration types was linked to greater decreases in SOM content through time ($r = 0.304$, $P = 0.032$, $n = 50$). Lower urease and GAP enzyme activities and lower relative AMF abundance were also linked to greater decreases in SOM content through time ($r = 0.333$, $P = 0.021$; $r = 0.297$, $P = 0.038$; $r = 0.251$, $P = 0.079$, respectively).

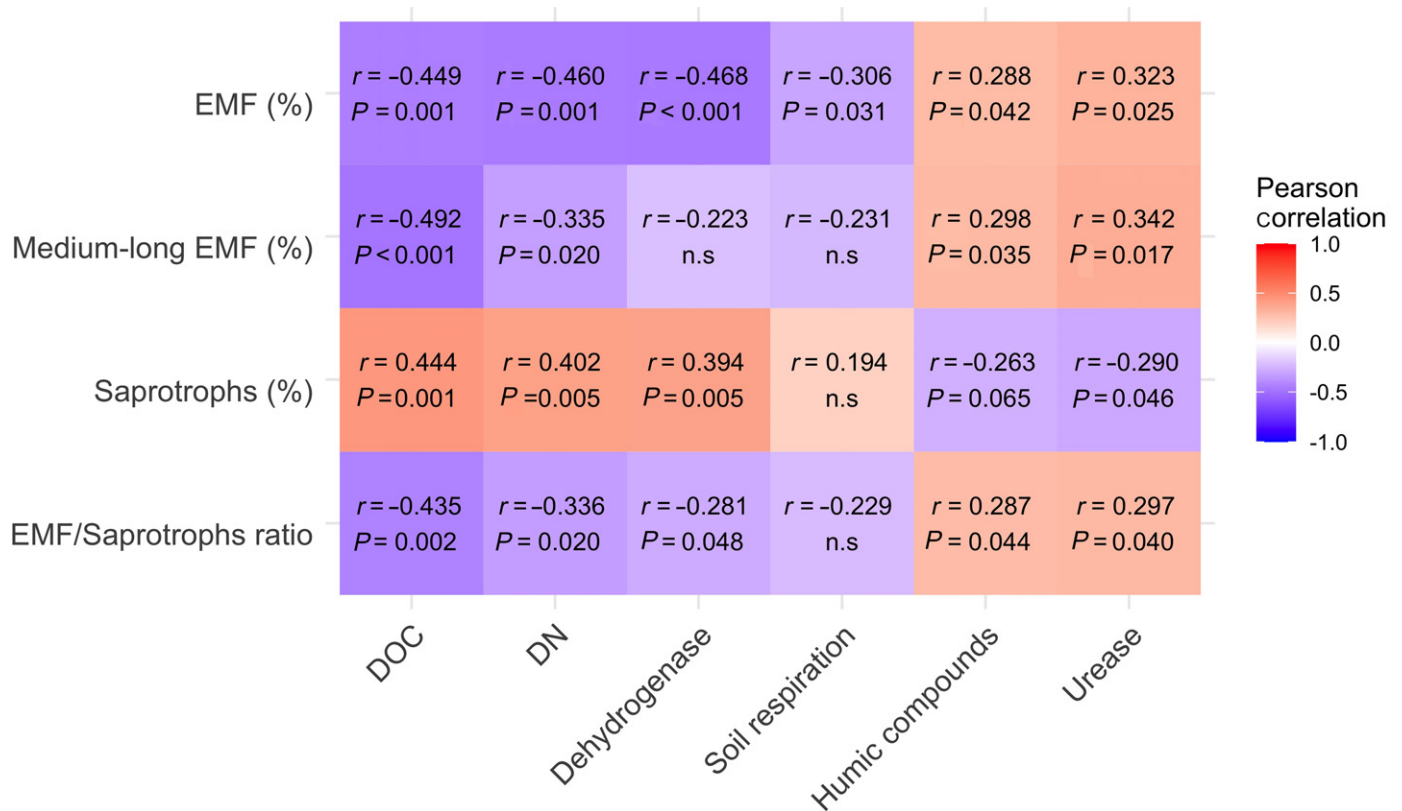


Fig. 5 Heatmap depicting Pearson correlations between fungal guild abundances and soil variables across climate treatments ($n = 50$). Fungal variables shown are: relative abundance of ectomycorrhizal fungi (EMF %); relative abundance of ectomycorrhizal fungi with medium-distance and long-distance hyphal exploration types (medium-long EMF %); relative abundance of saprotrophic fungi (saprotrophs %); the ratio of ectomycorrhizal/saprotrophs relative abundances (EMF/saprotrophs ratio). Soil properties shown are: dissolved organic carbon (DOC); dissolved nitrogen (DN); dehydrogenase enzyme activity (dehydrogenase); heterotrophic soil respiration (soil respiration); humic compounds content (humic compounds); urease enzyme activity (urease). Pairwise Pearson correlation coefficients (r) and P -values are shown. ns, not significant.

Discussion

We report a drastic change in the functional guild structure of the soil fungal community in a nutrient-poor semiarid shrubland exposed to simulated climate aridification. Greatly reduced EMF abundance under experimental climate warming combined with rainfall reduction (W+RR) was linked to increased saprotrophic fungal abundance along with enhanced SOM decomposition and N mineralisation. To our knowledge, this is the first study reporting a climate change-induced debilitation of the Gadgil effect that alters the ecosystem biogeochemistry and mycorrhizal-associated nutrient economy in drylands.

Climate change-induced increases in EM host plant mortality (60–70%) along with lower photosynthesis and growth of the stressed surviving plants (León-Sánchez *et al.*, 2020) may explain the sharp reduction in EMF abundance found under W+RR. Our inferences about changes in EMF and saprotrophic fungal abundance are based on relative abundances calculated from sequence read counts, which is similar to the approach used in other studies (Sterkenburg *et al.*, 2018). Despite the semiquantitative nature of this approach (Amend *et al.*, 2010), the data unequivocally revealed a drastic decrease in raw and relative EMF sequence abundance under simulated warmer and drier conditions, which is similar to the findings of another two independent climate change experiments from dryland ecosystems (León-Sánchez *et al.*, 2018; Gehring *et al.*, 2020). This result is also in agreement with the trend of decreasing EMF abundance encountered along aridity gradients in global drylands (Berdugo *et al.*, 2020). Our study is based on the assumption that the functional

guild structure of identified fungi (59.3% of fungal OTUs) is representative of unidentified fungi as well (40.7% of fungal OTUs), as customarily assumed (Fernandez *et al.*, 2020).

The drastic reduction of both raw and relative EMF abundances and diversity under W+RR was accompanied by a decreased activity of metabolically expensive hydrolytic enzymes involved in the acquisition of organic-bound N and P forms by EMF and their host plants (Courty *et al.*, 2005, 2010). A large proportion of the soil N and P content in nutrient-poor EM ecosystems is bound to SOM and therefore must be depolymerised by microbial extracellular enzymes before it can be taken up by roots. Warmer and drier conditions appeared to weaken the capacity of climatically stressed survivor EM host plants and their EMF symbionts for mining recalcitrant organic N and P sources bound in SOM (Bahram *et al.*, 2020). Survivor EM plants in the W+RR treatment showed 5–10% lower foliar N and P concentrations than those under current climate conditions, which further supports a decreased capacity for nutrient acquisition by roots and their EMF symbionts under a warmer and drier climate (León-Sánchez *et al.*, 2020).

Different EMF taxa showed contrasting vulnerability to simulated climate aridification, depending on their phylogeny and functional traits. We observed that EMF basidiomycetes with medium-distance and long-distance hyphal exploration types and metabolically expensive nutrient-acquiring enzymatic capabilities (*Scleroderma*, *Cortinarius*; Agerer, 2001) showed large decreases in their relative sequence abundances under warmer and drier climate conditions. Climatically stressed EM host plants may become less capable of sustaining the high carbon cost of these

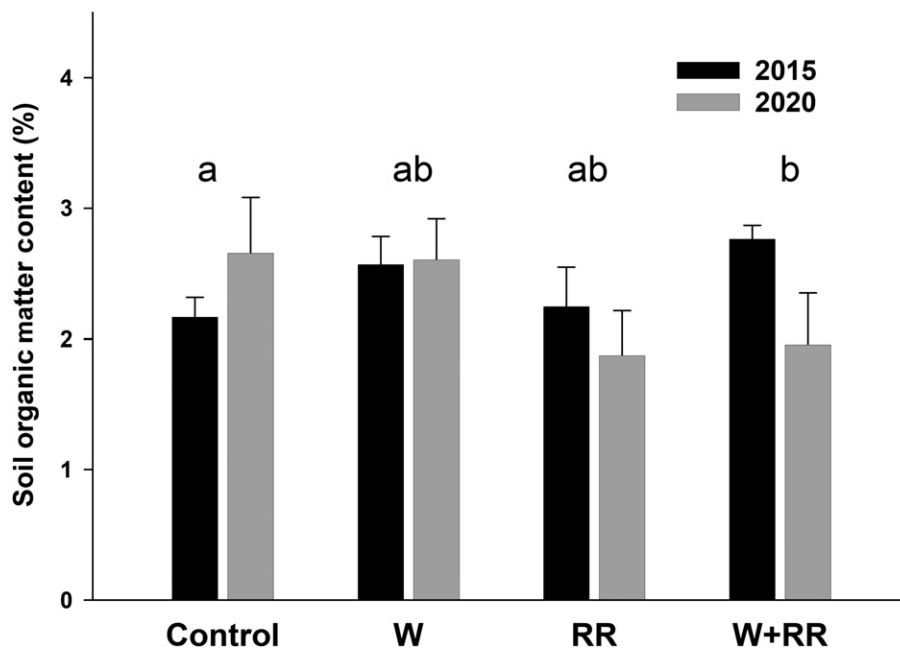


Fig. 6 Topsoil organic matter content (0–15 cm depth) measured 4 yr (2015, black columns) and 9 yr (2020, grey columns) since the start of the climate manipulation experiment in May 2011. Means and standard errors are shown ($n = 10–19$) for each climate treatment (Control; RR, rainfall reduction; W, warming; W+RR, warming plus rainfall reduction). Letters above columns represent the result of a multiple comparisons LSD test evaluating whether the change in soil organic matter content between 2015 and 2020 was significantly different between treatments ($P < 0.05$). Climate treatments sharing the same letters are not significantly different.

'expensive' EMF symbionts (Fernandez *et al.*, 2017) under more arid conditions. Climatically stressed survivor EM plants may instead be forced to rely on direct root nutrient uptake or other less carbon-demanding symbiotic partners such as ascomycete EMF with contact or short-distance hyphal exploration types and less complex enzymatic capabilities (*Geopora*). However, an important caveat is that root colonisation by different EMF was not assessed in our experiment, so further studies are needed to elucidate this aspect.

Partial competitive release from EMF and alleviation of nutrient limitation in free-living heterotrophic soil microbes could explain the shift towards a more saprotroph-dominated fungal community under W+RR. This shift in the competitive balance between the EMF and saprotrophic fungal guilds under W+RR may have decreased the strength of the Gadgil effect in this nutrient-poor ecosystem (Fernandez & Kennedy, 2016). A climate change-induced debilitation of the Gadgil effect creates an enhanced potential for the breakdown of stabilised SOM and nitrogen mineralisation by free-living fungal decomposers, as revealed by the two-fold and three-fold increases in DOC and DN contents, respectively, encountered under W+RR (Kalbitz *et al.*, 2000). Free-living microbial decomposers catalyse the conversion of polymeric SOM to DOC, which is the main rate-limiting step in SOM decomposition (Allison *et al.*, 2010). Drier soil and reduced leaching contributed to higher DOC contents with rainfall reduction and warming-induced soil desiccation, although the abundance of EMF sequences explained a larger proportion of variance in DOC than soil moisture (Table S8; Fig. S13). Conversely, the activity of free-living heterotrophic microbes can be enhanced by temperature elevation, so a general warming-induced stimulation of microbial activity may have further contributed to higher DOC in the W+RR treatment (Crowther *et al.*, 2016; Feng *et al.*, 2017; Bond-Lamberty *et al.*, 2018). However, there were no significant increases in DOC/DN contents or SOM decomposition in the W treatment despite the same temperature elevation as in W+RR. Enhanced soil DOC and DN contents and decreasing SOM content through time were only observed under W+RR, which suggests that they were specifically linked to the drastic reduction of EMF abundance coupled with increased fungal saprotroph abundance that was observed in the W+RR treatment only (Fig. 5). Overall, the changes in soil biogeochemistry and SOM content encountered under W+RR provide empirical support for the conceptual model outlined in Fig. 1, as higher EM host plant mortality and decreased EMF abundance were linked to enhanced DOC/DN production and SOM decomposition by saprotrophs under warmer and drier climatic conditions. We suggest that warming-induced and drought-induced decreases in EMF abundance could also lead to stimulation of SOM decomposition and N mineralisation through reductions in Gadgil effect strength at biome scale. The mixed EM/AM semiarid pinyon-juniper woodlands in the US Southwest would provide an ideal system for testing this hypothesis, as they are undergoing severe climate warming and drying linked to extensive mortality of EM pinyons (Mueller *et al.*, 2005, 2019).

The increase in the abundance of saprotrophic fungi under W+RR was accompanied by decreased diversity of the saprotrophic fungal guild, indicating that fewer taxa became dominant and were probably largely responsible for the enhanced decomposition of SOM in this treatment. Fungal decomposer communities generally show a negative diversity/decomposition rate relationship because coexisting saprotrophic fungi tend to be aggressively antagonistic towards each other (Toljander *et al.*, 2006; Fukami *et al.*, 2010). Dominance of the soil fungal community by free-living saprobes may favour immobilisation of limiting nutrients in the biomass of microbial decomposers under W+RR, which may decrease their availability to mycorrhizae and roots and therefore aggravate nutrient limitation of primary productivity with climate aridification (León-Sánchez *et al.*, 2020).

Our study provides the first indication of strong Gadgil effects in nutrient-poor shrublands, as this mechanism has been documented mainly in temperate and boreal conifer forests so far (Fernandez & Kennedy, 2016). The poor development and patchy spatial distribution of the thin litter layer in drylands do not favour vertical segregation between saprotrophic fungi and EMF (Lindahl *et al.*, 2007; Bödeker *et al.*, 2016), which may preclude niche partitioning and therefore may foster antagonistic interactions between these two competing guilds (Kvaschenko *et al.*, 2017). Moreover, semiarid shallow soils show poor vertical stratification of chemical and physical properties along the profile and high carbon-to-nutrient ratios in SOM and litter (Prieto & Querejeta, 2020; Querejeta *et al.*, 2021), which may further intensify competition for limiting resources between EMF and saprotrophic fungi (Fernandez *et al.*, 2020). The phylogeny and functional traits of EMF taxa may also play a key role in determining the strength of Gadgil effects, as dominance by basidiomycete EMF with medium-distance and long-distance hyphal exploration types and complex nutrient-acquiring enzymatic capabilities (*Scleroderma*, *Cortinari*) under current ambient conditions appeared to be most effective at suppressing the SOM decomposing activity of saprotrophic fungi. By contrast, ascomycete EMF with short-distance and contact hyphal exploration types (*Geopora*, *Picoa*, *Terfezia*) may be less effective at suppressing saprotrophic fungal activity, possibly because they are less aggressive competitors and colonisers of SOM.

Our data support the notion that AMF may be more tolerant and less vulnerable to heat and drought stress than EMF (Querejeta *et al.*, 2009; Vargas *et al.*, 2010; León-Sánchez *et al.*, 2018). The relative abundance of AMF sequences was highest under W+RR, which suggests that climatically stressed EM/AM *Helianthemum* plants could be forced to increasingly rely on AMF for nutrient acquisition with climate aridification, due to the lower carbon cost of this partnership for the host (Teste *et al.*, 2020). However, an important caveat is that the abundance of AMF sequences in the soil fungal community is underestimated when using universal fungal ITS primers (Schlaeppli *et al.*, 2016), so further studies using AMF-specific primers will be needed to elucidate this aspect. Another caveat is that AM root colonisation was not measured in our study. Moreover, our shrubland community includes several strict AM shrub and annual species growing side by side with *Helianthemum* shrubs within the same

vegetation patches, which confounds the interpretation of AMF sequence abundances. Interestingly, stepwise regression models (Table S8) revealed that soil DOC content decreased with increasing AMF sequence abundance across soil samples, which suggests a significant AMF contribution to the Gadgil effect in low-fertility drylands (Leifheit *et al.*, 2015).

Delgado-Baquerizo *et al.* (2014) reported that W+RR enhanced soil N mineralisation rates and dissolved inorganic and organic N contents in semiarid shrublands, as also reported here and widely observed globally (Bai *et al.*, 2013). Overall, the data suggest a climate change-induced shift in the mycorrhizal-associated nutrient economy of this shrubland from an EMF-dominated organic nutrient economy under the present climate scenario towards a more inorganic nutrient economy linked to enhanced rates of SOM decomposition and N mineralisation by free-living saprotrophs under W+RR. Increased availability of inorganic nutrients due to enhanced SOM decomposition should provide a competitive advantage to AM plants specialised in the uptake of inorganic N and P, at the expense of EM plants specialised in the utilisation of organic-bound N and P sources. This could eventually favour a progressive ecosystem transition towards a more AM-dominated inorganic nutrient economy in this mixed EM/AM shrubland with ongoing climate aridification (Phillips *et al.*, 2013; Jo *et al.*, 2019; Bahram *et al.*, 2020).

In conclusion, this study highlights how climate aridification impacts on aboveground vegetation cascade belowground through shifts in soil fungal guild abundance and biogeochemistry. The combination of experimental warming and drought increased EM host plant mortality and drastically reduced EMF abundance in a mixed EM/AM shrubland, which was linked to increased saprotrophic fungal abundance and enhanced SOM decomposition and N mineralisation. Our findings are in agreement with a recent meta-analysis demonstrating strong links between EMF abundance and soil carbon storage at global scale (Soudzilovskaia *et al.*, 2019), and have implications for predicting the responses of nutrient-poor EM/AM ecosystems to ongoing climate aridification. Climate change-induced shifts in fungal guild structure may contribute to accelerate SOM decomposition and CO₂ release from soil in low-fertility habitats, with potential detrimental consequences for soil carbon storage. Lower vegetation productivity under a warmer and drier climate may further hamper carbon storage through reductions in cumulative inputs of plant debris to soil and therefore reduced SOM build-up. A dwindling SOM content would lead to degradation of soil quality, given that SOM is a key parameter determining soil fertility, aggregation, infiltration, moisture retention capacity and vulnerability to erosion (Carter, 2002). Enhanced decomposition of SOM caused by a climate change-induced debilitation of the Gadgil effect could therefore entail a progressive decline of the water and nutrient retention capacity of low-fertility semiarid ecosystems that could further reduce vegetation productivity and survival, thereby accelerating dryland degradation and desertification processes under a warmer and drier climate.


Acknowledgements


We thank María José Espinosa, Jorge López, Roberto Lázaro, Fernando Maestre and Carlos García for help with field and laboratory work. Climate data were provided by AEMET. This study was funded by the Ministerio de Economía y Competitividad (projects CGL2010-21064 and CGL2013-48753-R co-funded by European Union FEDER funds) and Fundación Séneca (19477/PI/14). MdMA acknowledges a mobility fellowship funded by the 'José Castillejo' programme (CAS14/00023) of the Ministerio de Educación y Formación Profesional.


Author contributions


JIQ planned, designed and obtained funding for this research; JIQ, IP, MdMA performed the field experiments and conducted fieldwork; MdMA, KS, SO, MGAvdH conducted laboratory work; JIQ, MdMA, AL-G, KS, IP analysed the data; JIQ, MdMA, KS wrote the manuscript with feedback from all the co-authors. JIQ and MdMA contributed equally to this work.


ORCID


María del Mar Alguacil  <https://orcid.org/0000-0001-8495-8707>

Álvaro López-García  <https://orcid.org/0000-0001-8267-3572>

Sara Ondoño  <https://orcid.org/0000-0001-7992-8327>

Iván Prieto  <https://orcid.org/0000-0001-5549-1132>

José Ignacio Querejeta  <https://orcid.org/0000-0002-9547-0974>

Klaus Schlaeppi  <https://orcid.org/0000-0003-3620-0875>

Marcel G. A. van der Heijden  <https://orcid.org/0000-0001-7040-1924>

Data availability

The data that support the findings of this study are available from the corresponding author upon reasonable request.

References

- Abarenkov K, Henrik Nilsson R, Larsson K-H, Alexander IJ, Eberhardt U, Erland S, Høiland K, Kjoller R, Larsson E, Pennanen T *et al.* 2010. The UNITE database for molecular identification of fungi – recent updates and future perspectives. *New Phytologist* 186: 281–285.
- Agerer R. 2001. Exploration types of ectomycorrhizae - a proposal to classify ectomycorrhizal mycelial systems according to their patterns of differentiation and putative ecological importance. *Mycorrhiza* 11: 107–114.
- Allison SD, Wallenstein MD, Bradford MA. 2010. Soil-carbon response to warming dependent on microbial physiology. *Nature Geoscience* 3: 336–340.
- Amend AS, Seifert KA, Bruns TD. 2010. Quantifying microbial communities with 454 pyrosequencing: does read abundance count? *Molecular Ecology* 19: 5555–5565.
- Averill C, Hawkes CV. 2016. Ectomycorrhizal fungi slow soil carbon cycling. *Ecology Letters* 19: 937–947.
- Averill C, Turner BL, Finzi AC. 2014. Mycorrhiza-mediated competition between plants and decomposers drives soil carbon storage. *Nature* 505: 543–545.
- Bahram M, Netherway T, Hildebrand F, Pritsch K, Drenkhan R, Loit K, Anslan S, Bork P, Tedersoo L. 2020. Plant nutrient-acquisition strategies drive topsoil microbiome structure and function. *New Phytologist* 227: 1189–1199.

- Bai E, Li S, Xu W, Li W, Dai W, Jiang P. 2013. A meta-analysis of experimental warming effects on terrestrial nitrogen pools and dynamics. *New Phytologist* 199: 441–451.
- Bardgett RD, Hobbs PJ, Frostegård Å. 1996. Changes in soil fungal: bacterial biomass ratios following reductions in the intensity of management of an upland grassland. *Biology and Fertility of Soils* 22: 261–264.
- Bastida F, Torres IF, Andrés-Abellán M, Baldrian P, López-Mondéjar R, Větrovský T, Richnow HH, Starke R, Ondoño S, García C *et al.* 2017. Differential sensitivity of total and active soil microbial communities to drought and forest management. *Global Change Biology* 23: 4185–4203.
- Bennett AE, Classen AT. 2020. Climate change influences mycorrhizal fungal–plant interactions, but conclusions are limited by geographical study bias. *Ecology* 101: e02978.
- Berdugo M, Delgado-Baquerizo M, Soliveres S, Hernández-Clemente R, Zhao Y, Gaitán JJ, Gross N, Saiz H, Maire V, Lehmann A *et al.* 2020. Global ecosystem thresholds driven by aridity. *Science* 367: 787–790.
- Bödeker ITM, Lindahl BD, Olson Å, Clemmensen KE. 2016. Mycorrhizal and saprotrophic fungal guilds compete for the same organic substrates but affect decomposition differently. *Functional Ecology* 30: 1967–1978.
- Bond-Lamberty B, Bailey VL, Chen M, Gough CM, Vargas R. 2018. Globally rising soil heterotrophic respiration over recent decades. *Nature* 560: 80–83.
- Brundrett MC. 2009. Mycorrhizal associations and other means of nutrition of vascular plants: understanding the global diversity of host plants by resolving conflicting information and developing reliable means of diagnosis. *Plant and Soil* 320: 37–77.
- Caporaso JG, Kuczynski J, Stombaugh J, Bittinger K, Bushman FD, Costello EK, Fierer N, Peña AG, Goodrich JK, Gordon JI *et al.* 2010. QIIME allows analysis of high-throughput community sequencing data. *Nature Methods* 7: 335–336.
- Carter MR. 2002. Soil quality for sustainable land management. *Agronomy Journal* 94: 38–47.
- Clemmensen KE, Bahr A, Ovaskainen O, Dahlberg A, Ekblad A, Wallander H, Stenlid J, Finlay RD, Wardle DA, Lindahl BD. 2013. Roots and associated fungi drive long-term carbon sequestration in boreal forest. *Science* 339: 1615–1618.
- Coleman MD, Bledsoe CS, Lopushinsky W. 1989. Pure culture response of ectomycorrhizal fungi to imposed water stress. *Canadian Journal of Botany* 67: 29–39.
- Comandini O, Contu M, Rinaldi AC. 2006. An overview of *Cistus* ectomycorrhizal fungi. *Mycorrhiza* 16: 381–395.
- Compant S, Van Der Heijden MGA, Sessitsch A. 2010. Climate change effects on beneficial plant–microorganism interactions. *FEMS Microbiology Ecology* 73: 197–214.
- Courty PE, Buée M, Diedhou AG, Frey-Klett P, Le Tacon F, Rineau F, Turpault MP, Uroz S, Garbaye J. 2010. The role of ectomycorrhizal communities in forest ecosystem processes: new perspectives and emerging concepts. *Soil Biology and Biochemistry* 42: 679–698.
- Courty PE, Pritsch K, Schloter M, Hartmann A, Garbaye J. 2005. Activity profiling of ectomycorrhiza communities in two forest soils using multiple enzymatic tests. *New Phytologist* 167: 309–319.
- Crowther TW, Todd-Brown K, Rowe CW, Wieder WR, Carey JC, Machmuller MB, Snoek BL, Fang S, Zhou G, Allison SD *et al.* 2016. Quantifying global soil carbon losses in response to warming. *Nature* 540: 104–108.
- Delgado-Baquerizo M, Maestre FT, Escolar C, Gallardo A, Ochoa V, Gozalo B, Prado-Comesaña A. 2014. Direct and indirect impacts of climate change on microbial and biocrust communities alter the resistance of the N cycle in a semiarid grassland. *Journal of Ecology* 102: 1592–1605.
- Edgar RC. 2013. UPARSE: highly accurate OTU sequences from microbial amplicon reads. *Nature Methods* 10: 996–998.
- Edgar RC, Haas BJ, Clemente JC, Quince C, Knight R. 2011. UCHIME improves sensitivity and speed of chimera detection. *Bioinformatics* 27: 2194–2200.
- Feng W, Liang J, Hale LE, Jung CG, Chen Ji, Zhou J, Xu M, Yuan M, Wu L, Bracho R *et al.* 2017. Enhanced decomposition of stable soil organic carbon and microbial catabolic potentials by long-term field warming. *Global Change Biology* 23: 4765–4776.
- Fernandez CW, Kennedy PG. 2016. Revisiting the ‘Gadgil effect’: do interguild fungal interactions control carbon cycling in forest soils? *New Phytologist* 209: 1382–1394.
- Fernandez CW, Nguyen NH, Stefanski A, Han Y, Hobbie SE, Montgomery RA, Reich PB, Kennedy PG. 2017. Ectomycorrhizal fungal response to warming is linked to poor host performance at the boreal-temperate ecotone. *Global Change Biology* 23: 1598–1609.
- Fernandez CW, See CR, Kennedy PG. 2020. Decelerated carbon cycling by ectomycorrhizal fungi is controlled by substrate quality and community composition. *New Phytologist* 226: 569–582.
- Frey SD. 2019. Mycorrhizal fungi as mediators of soil organic matter dynamics. *Annual Review of Ecology Evolution and Systematics* 50: 237–259.
- Frostegård A, Baath E. 1996. The use of phospholipid fatty acid analysis to estimate bacterial and fungal biomass in soil. *Biology and Fertility of Soils* 22: 59–65.
- Fukami T, Dickie IA, Wilkie JP, Paulus BC, Park D, Roberts A, Buchanan PK, Allen RB. 2010. Assembly history dictates ecosystem functioning: evidence from wood decomposer communities. *Ecology Letters* 13: 675–684.
- Gadgil RL, Gadgil PD. 1971. Mycorrhiza and litter decomposition. *Nature* 233: 133.
- García C, Hernandez T, Costa F. 1994. Microbial activity in soils under Mediterranean environmental conditions. *Soil Biology and Biochemistry* 26: 1185–1191.
- Gardes M, Bruns TD. 1993. ITS primers with enhanced specificity for basidiomycetes - application to the identification of mycorrhizae and rusts. *Molecular Ecology* 2: 113–118.
- Gehring C, Sevanto S, Patterson A, Ulrich DEM, Kuske CR. 2020. Ectomycorrhizal and dark septate fungal associations of pinyon pine are differentially affected by experimental drought and warming. *Frontiers in Plant Science* 11: 582574.
- Giorgi F, Lionello P. 2008. Climate change projections for the Mediterranean region. *Global and Planetary Change* 63: 90–104.
- Guiot J, Cramer W. 2016. Climate change: the 2015 Paris Agreement thresholds and Mediterranean basin ecosystems. *Science* 354: 465–468.
- Guo LB, Gifford RM. 2002. Soil carbon stocks and land use change: a meta analysis. *Global Change Biology* 8: 345–360.
- Hacker N, Ebeling A, Gessler A, Gleixner G, González Macé O, de Kroon H, Lange M, Mommer L, Eisenhauer N, Ravenek J *et al.* 2015. Plant diversity shapes microbe-rhizosphere effects on P mobilisation from organic matter in soil. *Ecology Letters* 18: 1356–1365.
- Hartman K, van der Heijden MGA, Wittwer RA, Banerjee S, Walser JC, Schlaeppi K. 2018. Cropping practices manipulate abundance patterns of root and soil microbiome members paving the way to smart farming. *Microbiome* 6: 14.
- Hollister RD, Weber PJ. 2000. Biotic validation of small open-top chambers in a tundra ecosystem. *Global Change Biology* 6: 835–842.
- Jo I, Fei S, Oswalt CM, Domke GM, Phillips RP. 2019. Shifts in dominant tree mycorrhizal associations in response to anthropogenic impacts. *Science Advances* 5: eaav6358.
- Kalbitz K, Solinger S, Park JH, Michalzik B, Matzner E. 2000. Controls on the dynamics of dissolved organic matter in soils: a review. *Soil Science* 165: 277–304.
- Kandeler E, Palli S, Stemmer M, Gerzabek MH. 1999. Tillage changes microbial biomass and enzyme activities in particle-size fractions of a Haplic Chernozem. *Soil Biology and Biochemistry* 31: 1253–1264.
- Kyaschenko J, Clemmensen KE, Karlton E, Lindahl BD. 2017. Below-ground organic matter accumulation along a boreal forest fertility gradient relates to guild interaction within fungal communities. *Ecology Letters* 20: 1546–1555.
- Leifheit EF, Verbruggen E, Rillig MC. 2015. Arbuscular mycorrhizal fungi reduce decomposition of woody plant litter while increasing soil aggregation. *Soil Biology and Biochemistry* 81: 323–328.
- Leonardi M, Neves MA, Comandini O, Rinaldi AC. 2018. *Scleroderma meridionale* ectomycorrhizae on *Halimium halimifolium*: expanding the Mediterranean symbiotic repertoire. *Symbiosis* 76: 199–208.
- León-Sánchez L, Nicolás E, Goberna M, Prieto I, Maestre FT, Quesada JL. 2018. Poor plant performance under simulated climate change is linked to mycorrhizal responses in a semi-arid shrubland. *Journal of Ecology* 106: 960–976.

- León-Sánchez L, Nicolás E, Prieto I, Nortes P, Maestre FT, Querejeta JI. 2020. Altered leaf elemental composition with climate change is linked to reductions in photosynthesis, growth and survival in a semi-arid shrubland. *Journal of Ecology* 108: 47–60.
- Lindahl BD, Finlay RD, Cairney JWG. 2005. Enzymatic activities of mycelia in mycorrhizal fungal communities. In: Dighton J, White JF, Oudemans P, eds. *The fungal community: its organization and role in the ecosystem*, 3rd edn. Boca Raton, FL, USA: CRC Press, 331–348.
- Lindahl BD, Ihrmark K, Boberg J, Trumbore SE, Högberg P, Stenlid J, Finlay RD. 2007. Spatial separation of litter decomposition and mycorrhizal nitrogen uptake in a boreal forest. *New Phytologist* 173: 611–620.
- Magoc T, Salzberg SL. 2011. FLASH: Fast length adjustment of short reads to improve genome assemblies. *Bioinformatics* 21: 2957–2963.
- Marqués-Gálvez JE, Morte A, Navarro-Ródenas A. 2020. Spring stomatal response to vapor pressure deficit as a marker for desert truffle fruiting. *Mycorrhiza* 30: 503–512.
- Martin M. 2011. Cutadapt removes adapter sequences from high-throughput sequencing reads. *EMBnet Journal* 17: 10–12.
- McGuire KL, Payne SG, Palmer MI, Gillikin CM, Keefe D, Kim SJ, Gedalovich SM, Discenza J, Rangamannar R, Koshner JA *et al.* 2013. Digging the New York city skyline: soil fungal communities in green roofs and city parks. *PLoS ONE* 8: e58020.
- Mueller RC, Scudder CM, Porter ME, Talbot R, Gehring CA, Whitham CA. 2005. Differential tree mortality in response to severe drought: evidence for long-term vegetation shifts. *Journal of Ecology* 93: 1085–1093.
- Mueller RC, Scudder CM, Whitham TG, Gehring CA. 2019. Legacy effects of tree mortality mediated by ectomycorrhizal fungal communities. *New Phytologist* 224: 155–165.
- Nguyen NH, Song Z, Bates ST, Branco S, Tedersoo L, Menke J, Schilling JS, Kennedy PG. 2016. FUNGuild: An open annotation tool for parsing fungal community datasets by ecological guild. *Fungal Ecology* 20: 241–248.
- Nickel UT, Weigl F, Kerner R, Schäfer C, Kallenbach C, Munch JC, Pritsch K. 2018. Quantitative losses vs. qualitative stability of ectomycorrhizal community responses to 3 years of experimental summer drought in a beech–spruce forest. *Global Change Biology* 24: e560–e576.
- Oksanen J, Blanchet FG, Kindt R, Legendre P, Minchin PR, O'Hara RB, Simpson GL, Solymos P, Stevens MHH, Wagner HH. 2016. *Vegan: community ecology package*. R package v.2.4-10. [WWW document] URL <https://CRAN.R-project.org/package=vegan>.
- Orwin KH, Kirschbaum MUF, St John MG, Dickie IA. 2011. Organic nutrient uptake by mycorrhizal fungi enhances ecosystem carbon storage: a model-based assessment. *Ecology Letters* 14: 493–502.
- Perez-Moreno J, Read DJ. 2000. Mobilization and transfer of nutrients from litter to tree seedlings via the vegetative mycelium of ectomycorrhizal plants. *New Phytologist* 145: 301–309.
- Phillips RP, Brzostek E, Midgley MG. 2013. The mycorrhizal-associated nutrient economy: a new framework for predicting carbon–nutrient couplings in temperate forests. *New Phytologist* 199: 41–51.
- Prieto I, Almagro M, Bastida F, Querejeta JI. 2019. Altered leaf litter quality exacerbates the negative impact of climate change on decomposition. *Journal of Ecology* 107: 2364–2382.
- Prieto I, Querejeta JI. 2020. Simulated climate change decreases nutrient resorption from senescing leaves. *Global Change Biology* 26: 1795–1807.
- Pritsch K, Garbaye J. 2011. Enzyme secretion by ECM fungi and exploitation of mineral nutrients from soil organic matter. *Annals of Forest Science* 68: 25–32.
- Querejeta JI, Egerton-Warburton LM, Allen MF. 2009. Topographic position modulates the mycorrhizal response of oak trees to interannual rainfall variability. *Ecology* 90: 649–662.
- Querejeta JI, Ren W, Prieto I. 2021. Vertical decoupling of soil nutrients and water under climate warming reduces plant cumulative nutrient uptake, water use efficiency and productivity. *New Phytologist* 230: 1378–1393.
- Quilchano C, Marañón T. 2002. Dehydrogenase activity in Mediterranean forest soils. *Biology & Fertility of Soils* 35: 102–107.
- R Core Team. 2019. *R: a language and environment for statistical computing*. Vienna, Austria: R Foundation for Statistical Computing.
- Read DJ, Perez-Moreno J. 2003. Mycorrhizas and nutrient cycling in ecosystems – a journey towards relevance? *New Phytologist* 157: 475–492.
- Ross DJ. 1971. Some factors affecting the estimation of dehydrogenase activities of some soils under pasture. *Soil Biology and Biochemistry* 3: 97–110.
- Schimel JP, Bennett J. 2004. Nitrogen mineralization: challenges of a changing paradigm. *Ecology* 85: 591–602.
- Schlaeppli K, Bender SF, Mascher F, Russo G, Patrignani A, Camenzind T, Hempel S, Rillig MC, van der Heijden MGA. 2016. High-resolution community profiling of arbuscular mycorrhizal fungi. *New Phytologist* 212: 780–791.
- Schmieder R, Edwards R. 2011. Quality control and preprocessing of metagenomic datasets. *Bioinformatics* 27: 863–864.
- Soudzilovskaia NA, van Bodegom PM, Terrer C, Zelfde MV, McCallum I, McCormack ML, Fisher JB, Brundrett MC, de Sá NC, Tedersoo L. 2019. Global mycorrhizal plant distribution linked to terrestrial carbon stocks. *Nature Communications* 10: 5077.
- Sterkenburg E, Clemmensen KE, Ekblad A, Finlay RD, Lindahl BD. 2018. Contrasting effects of ectomycorrhizal fungi on early and late stage decomposition in a boreal forest. *ISME Journal* 12: 2187.
- Stevenson FJ. 1985. Geochemistry of soil humic substances. In: Aiken GR, Mcknight DM, Wershaw RL, Mccarthy P, eds. *Humic substances in soil, sediment and water*. New York, NY, USA: John Wiley & Sons, 13–52.
- Swaty RL, Deckert RJ, Whitham TG, Gehring CA. 2004. Ectomycorrhizal abundance and community composition shifts with drought: predictions from tree rings. *Ecology* 85: 1072–1084.
- Swaty RL, Gehring CA, van Ert M, Theimer TC, Keim P, Whitham TG. 1998. Temporal variation in temperature and rainfall differentially affects ectomycorrhizal colonization at two contrasting sites. *New Phytologist* 139: 733–739.
- Tabatabai MA, Bremner JM. 1969. Use of p-nitrophenyl phosphate for assay of soil phosphatase activity. *Soil Biology and Biochemistry* 1: 301–307.
- Tedersoo L, Bahram M. 2019. Mycorrhizal types differ in ecophysiology and alter plant nutrition and soil processes. *Biological Reviews* 94: 1857–1880.
- Teste FP, Jones MD, Dickie IA. 2020. Dual-mycorrhizal plants: their ecology and relevance. *New Phytologist* 225: 1835–1851.
- Toljander JF, Eberhardt U, Toljander YK, Paul LR, Taylor AF. 2006. Species composition of an ectomycorrhizal fungal community along a local nutrient gradient in a boreal forest. *New Phytologist* 170: 873–884.
- Trevors JT, Mayfield CI, Inniss WE. 1982. Measurement of electron transport system (ETS) activity in soil. *Microbial Ecology* 8: 163–168.
- Vargas R, Baldocchi DD, Querejeta JI, Curtis PS, Hasselquist NJ, Janssens IA, Allen MF, Montagnani L. 2010. Ecosystem CO₂ fluxes of arbuscular and ectomycorrhizal dominated vegetation types are differentially influenced by precipitation and temperature. *New Phytologist* 185: 226–236.
- Wang T, Tian Z, Bengtson P, Tunlid A, Persson P. 2017. Mineral surface-reactive metabolites secreted during fungal decomposition contribute to the formation of soil organic matter. *Environmental Microbiology* 19: 5117–5129.
- White TJ, Bruns T, Lee S, Taylor J. 1990. Amplification and direct sequencing of fungal ribosomal RNA genes for phylogenetics. In: Innis MA, Gelfand DH, Sninsky JJ, White TJ, eds. *PCR protocols. A guide to methods and applications*. San Diego, CA, USA: Academic Press, 315–322.
- Yuste JC, Peñuelas J, Estiarte M, Garcia-Mas J, Mattana S, Ogaya R, Pujol M, Sardans J. 2011. Drought-resistant fungi control soil organic matter decomposition and its response to temperature. *Global Change Biology* 17: 1475–1486.
- Zak DR, Pellitier PT, Argiroff W, Castillo B, James TY, Nave LE, Averill C, Beidler KV, Bhatnagar J, Blesh J *et al.* 2019. Exploring the role of ectomycorrhizal fungi in soil carbon dynamics. *New Phytologist* 223: 33–39.
- Zuo Y, Li J, Zeng H, Wang W. 2018. Vertical pattern and its driving factors in soil extracellular enzyme activity and stoichiometry along mountain grassland belts. *Biogeochemistry* 141: 23–39.

Supporting Information

Additional Supporting Information may be found online in the Supporting Information section at the end of the article.

Fig. S1 Experimental plot exposed to the combination of warming and rainfall reduction (W+RR).

Fig. S2 Rarefaction curves on the rarefied operational taxonomic units dataset.

Fig. S3 Relative abundances of sequences belonging to the main fungal phyla and classes.

Fig. S4 Redundancy analysis (RDA) based on Hellinger distance matrix depicting the influence of the climate treatments on soil fungal community structure at operational taxonomic unit level.

Fig. S5 Relative sequence abundances of dominant fungal taxa within the ectomycorrhizal fungal and saprotrophic fungal guilds.

Fig. S6 Relative sequence abundances within the saprotrophic fungal guild grouped by major fungal phyla or grouped by growth form.

Fig. S7 Mean raw sequence abundances of ectomycorrhizal fungal and saprotrophic fungi in the different climate treatments.

Fig. S8 Relative abundances of arbuscular mycorrhizal fungi sequences grouped by families.

Fig. S9 Soil water content at time of sampling.

Fig. S10 Specific activities of extracellular nutrient-acquiring enzymes in rhizosphere soil.

Fig. S11 Humic compounds content in soil.

Fig. S12 Negative relationship between soil dissolved organic carbon content and the relative abundance of ectomycorrhizal fungal sequences across climate treatments.

Fig. S13 Negative relationship between soil scores along principal component analyses axis one and the relative abundance of ectomycorrhizal fungal across climate treatments.

Fig. S14 Structural equation model (SEM) based on the hypothesised effects of warming and rainfall reduction on soil moisture and relative abundance of ectomycorrhizal fungal and subsequent

effects on dissolved organic carbon and dissolved nitrogen contents in soil.

Methods S1 Barcodes and primers for raw sequence data.

Methods S2 Bioinformatics pipeline for processing raw sequence reads.

Methods S3 R script used for permutational multivariate analysis of variance and redundancy analysis analyses of fungal sequences.

Methods S4 List of references used for manual assignment of 60 fungal operational taxonomic units to functional guilds.

Table S1 Main soil properties at the study site.

Table S2 Permutational multivariate analysis of variance testing the effects of the climate manipulation treatments on soil fungal community structure.

Table S3 Diversity indexes for the entire soil fungal community and the ectomycorrhizal and saprotrophic fungal guilds.

Table S4 Two-way ANOVAs testing the effects of the experimental climate factors on the relative abundances of fungal sequences belonging to eight main functional guilds.

Table S5 Two-way ANOVAs testing the effects of the experimental climate factors on key soil properties.

Table S6 Mean microbial biomass, content, dehydrogenase enzyme activity and microbial heterotrophic respiration rate in rhizosphere soil.

Table S7 Principal component analysis of dissolved organic carbon content, dissolved nitrogen content, dehydrogenase enzyme activity and microbial heterotrophic respiration rate in soil samples.

Table S8 Regression models explaining variation in dissolved organic carbon and dissolved nitrogen contents in soil.

Please note: Wiley Blackwell are not responsible for the content or functionality of any Supporting Information supplied by the authors. Any queries (other than missing material) should be directed to the *New Phytologist* Central Office.